AD-A049 764 SOUTH DAKOTA SCHOOL OF MINES AND TECHNOLOGY RAPID CI--ETC F/G 11/6
AN INVESTIGATION OF THE INFLUENCE OF SHOCK-WAVE PROFILE ON THE --ETC(U)
JUN 77 G A STONE, R N ORAVA DAAG29-76-G-0181

UNCLASSIFIED ARO-12800.1-MSX NL

| OF |
AD A049764

END
DATE FILMED
3-78
DDC

ARO Grant No. DAAG29-76-G-0181 June 30, 1977

AN INVESTIGATION OF THE INFLUENCE OF SHOCK-WAVE PROFILE ON THE MECHANICAL AND THERMAL RESPONSES OF POLYCRYSTALLINE IRON

Interim Technical Report

Prepared For: U. S. Army Research Office - Durham
Box CM, Duke Station
Durham, NC 27706

Prepared By: G. A. Stone, R. N. Orava
Department of Metallurgical Engineering

New 410558

Division of Engineering,
South Dakota School of Mines & Technology
Rapid City, South Dakota 57701

Unclassified
SECURITY CLASSIFICATION OF THIS PAGE (When Data Entered) ARO 12800.1-MSX

REPORT DOCUMENTATION PAGE

READ INSTRUCTIONS BEFORE COMPLETING FORM

1. REPORT NUMBER (18) ARO (19) 12800.1-MSX
2. GOVT ACCESSION NO.
3. RECIPIENT'S CATALOG NUMBER
4. TITLE (and Subtitle) (6) An Investigation of the Influence of Shock-Wave Profile on the Mechanical and Thermal Responses of Polycrystalline Iron
5. TYPE OF REPORT & PERIOD COVERED (9) Interim Technical Report
6. PERFORMING ORG. REPORT NUMBER
7. AUTHOR(s) (10) G. A. Stone, R. N. Orava
8. CONTRACT OR GRANT NUMBER(s) (15) DAAG29-76-G-0181 new
9. PERFORMING ORGANIZATION NAME AND ADDRESS
South Dakota School of Mines & Technology
Division of Engineering
Rapid City, South Dakota 57701
10. PROGRAM ELEMENT, PROJECT, TASK AREA & WORK UNIT NUMBERS
11. CONTROLLING OFFICE NAME AND ADDRESS
U. S. Army Research Office
Post Office Box 12211
Research Triangle Park, NC 27709
12. REPORT DATE Jun 77 (11) 30 Jun 77
13. NUMBER OF PAGES 40 (12) 45p.
14. MONITORING AGENCY NAME & ADDRESS (if different from Controlling Office)
15. SECURITY CLASS. (of this report) Unclassified
15a. DECLASSIFICATION/DOWNGRADING SCHEDULE

16. DISTRIBUTION STATEMENT (of this Report)

Approved for public release; distribution unlimited.

17. DISTRIBUTION STATEMENT (of the abstract entered in Block 20, if different from Report)

18. SUPPLEMENTARY NOTES

The findings in this report are not to be construed as an official Department of the Army position, unless so designated by other authorized documents.

19. KEY WORDS (Continue on reverse side if necessary and identify by block number)

Shock waves	Pressure	Thermal response
Mechanical properties	Microstructure	
Iron	Rarefaction	
Iron alloys	Phase transformations	

20. ABSTRACT (Continue on reverse side if necessary and identify by block number)

The purpose of this investigation is to study the influence of the shock-wave profile on the mechanical response of polycrystalline iron. The objective of this Interim Technical Report is to provide information in regard to significant progress made in this study. The three shock-wave parameters associated with the shock-wave profile are peak pressure, duration of peak pressure, and rarefaction rate. It is now evident that the major parameter of importance in developing mechanical properties in shock-loaded low carbon iron alloys is peak pressure. Pressure duration plays a role in the 13 to 33 GPa pressure →OVER

DD FORM 1 JAN 73 1473 EDITION OF 1 NOV 65 IS OBSOLETE

Unclassified 410 558 JOB
SECURITY CLASSIFICATION OF THIS PAGE (When Data Entered)

20. ABSTRACT CONTINUED

range for durations less than 1 μsec. Below 13 GPa and above 33 GPa the mechanical properties developed were not sensitive to the peak pressure durations used in the study. The $\alpha \rightarrow \varepsilon \rightarrow \alpha$ phase transformation is playing such a major role in microstructure development above 13 GPa that any modification to structure associated with rarefaction rate is a second order contribution. This study validates previous work on shock loading of iron where rarefaction rate was not considered.

Interim Technical Report

on

AN INVESTIGATION OF THE INFLUENCE OF SHOCK-WAVE PROFILE ON THE MECHANICAL AND THERMAL RESPONSES OF POLYCRYSTALLINE IRON

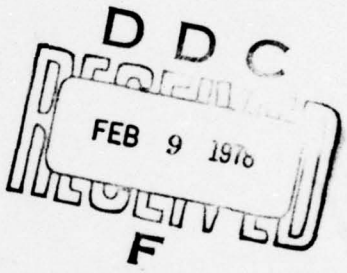

by

G. A. Stone, R. N. Orava,

Department of Metallurgical Engineering

South Dakota School of Mines and Technology

June 30, 1977

Prepared for

U. S. Army Research Office - Durham

ARO Grant No. DAAG29-76-G-0181

TABLE OF CONTENTS

Abstract

The purpose of this investigation is to study the influence of the shock-wave profile on the mechanical response of polycrystalline iron. The objective of this Interim Technical Report is to provide information in regard to significant progress made in this study.

The three shock-wave parameters associated with the shock-wave profile are peak pressure, duration of peak pressure, and rarefaction rate. It is now evident that the major parameter of importance in developing mechanical properties in shock-loaded low carbon iron alloys is peak pressure. Pressure duration plays a role in the 13 to 33 GPa pressure range for durations less than 1 μsec. Below 13 GPa and above 33 GPa the mechanical properties developed were not sensitive to the peak pressure durations used in the study.

The $\alpha \rightarrow \varepsilon \rightarrow \alpha$ phase transformation is playing such a major role in microstructure development above 13 GPa that any modification to structure associated with rarefaction rate is a second order contribution.

This study validates previous work on shock loading of iron where rarefaction rate was not considered.

I. Introduction

The purpose of this Interim Technical Report is to report all experimental results obtained to date and relate these results to several program objectives. A detailed discussion of the results will not be presented in this report.

1.1 Program Objectives

The purpose of this investigation is to study the influence of shock-wave profile on the mechanical response of polycrystalline iron. The objectives are:

1. To permit the classification of shock-wave parameters according to the order of their contribution in controlling: substructure, microstructure, and hardening. See Section 1.2.1 of report.
2. To assess the validity of previous results pertaining to the pressure dependence of the response of pure iron to shock loading. See Section 1.2.2 of report.
3. To contribute to the fundamental basis for the selection of wave profiles for optimum response. See Section 1.2.3 of report.
4. To correlate specific shock wave parameters with hardening, dislocation substructure, and $\alpha \rightarrow \varepsilon \rightarrow \alpha$ transformation.
5. To evaluate the response of shocked iron to strain aging as a result of shock loading.
6. To determine the extent of dynamic, or transient, strain aging as a result of the adiabatic temperature rise.
7. To improve the mechanistic understanding of the shock strengthening of iron, as it is affected by shock parameters other than peak pressure.

1.2 Objectives Achieved

1.2.1 Classification of Shock-Wave Parameters

The classification of the three shock-wave parameters, rarefaction rate, duration of peak pressure, and peak pressure, according to their contribution in controlling microstructure and hardening, has been completed. It is now clear that rarefaction rate has no systematic effect on the resulting microstructural and mechanical properties of low-carbon iron and steel. This result is not consistent with observation on nickel in the same pressure range, where mechanical properties and microstructure are influenced by rarefaction rate.[1] It is felt the $\alpha \rightarrow \varepsilon \rightarrow \alpha$ phase transformation that exists in iron plays such an enormous role in microstructure and substructure development that no measurable contribution by the rarefaction rate parameter results.

The shock-wave parameter, peak pressure duration, is important in developing material properties for short times (< 1 μsec). Above 1 μsec peak pressure duration, no systematic modifications of microstructure or mechanical properties were observed.

The peak pressure and the associated $\alpha \rightarrow \varepsilon \rightarrow \alpha$ phase transformation appear to be the dominant factors in the development of the observed microstructure and resulting mechanical properties. A two-fold increase in the ultimate tensile strength (UTS) resulted for AISI 1008 Steel and Armco Magnetic Ingot Iron, shock loaded at 25 and 35 GPa peak pressure.

1.2.2 Validity of Previous Results on Iron

It appears that previous studies on iron where no consideration for rarefaction rate were made are valid. These results are valid because the $\alpha \rightarrow \varepsilon \rightarrow \alpha$ phase transformation and the peak pressure are responsible for microstructure development. Any additional modifications to the materials microstructure due to the rarefaction rate appear to be second order effects

and were not resolvable in this study.

The duration of the peak pressure is important and must be reported for studies on the influence of shock waves in iron and steel. The current results suggest that significant modification of the microstructure are observed for short durations of the peak pressure (< 1 μsec). When the peak pressure duration is not reported, the validity of the data should be questioned.

1.2.3 Selection of Wave Profiles for Optimum Response

Results from this study are in good agreement with previous data.[2,3] These results show a rapid increase in hardness in iron and steel that is shock loaded at peak pressures above 13 GPa, reaching a maximum hardness when subjected to peak pressures near 25 GPa. When specimens are shock loaded above 35 GPa peak pressure, a general small decrease in hardness is observed with increasing peak pressure.

It is concluded that optimum mechanical properties are obtained in iron and steel when shock loaded between 25 and 35 GPa peak pressure and a peak pressure duration of 1 μsec.

1.3 Work in Progress

Isochronal treatments of shock-hardened material and cold-rolled material, rolled to the same maximum shear strain (as the shock-loaded material) are in progress. The objective is to establish the recrystallization temperature as a function of shock-loaded and cold-rolled properties. When this phase is complete, a systematic aging study in the recovery temperature range will be started. The objective of the aging study is to establish the optimum aging time and temperature that will reduce the mechanical instability observed in shock hardened materials and at the same time retain as much of the strength increase associated with shock hardening as possible.

The substructure study is progressing slowly. The objective of this phase of the program is to develop an assessment of the effects of the three shock-wave parameters; peak pressure, peak pressure duration and rarefaction rate on the residual substructure present in AISI 1008 steel and Armco Magnetic Ingot Iron.

II. Experimental Materials and Procedures

2.1 Materials

The materials under investigation were Armco Magnetic Ingot Iron and AISI 1008 Steel. Magnetic Ingot Iron sheet, 0.110 in. (2.8 mm) thick, was obtained from Armco Steel Corporation in a cold-rolled form. The AISI 1008 sheet of thickness 0.118 in. (3.0 mm) was received in a recrystallized form from the supplier.

The chemical analyses of the Ingot Iron and AISI 1008 Steel as determined by Anamet Laboratories, Inc., Berkeley, California are (weight percent):

Element	Ingot Iron	1008
Al	0.07	0.003
C	0.006	0.074
Cr	0.05	<0.005
Cu	0.11	<0.005
Mn	0.14	0.39
Mo	0.04	0.02
Ni	0.07	<0.005
N	0.006	0.002
O	0.004	0.007
P	0.006	0.007
Si	0.08	<0.005
S	0.019	0.010
Ti	0.07	<0.005

The Magnetic Ingot Iron was cut into three inch (7.5 cm) by four inch (10.2 cm) pieces, annealed at 723°C for one-half hour in an Argon atmosphere, and allowed to furnace cool. The average grain diameters were 19.3 micrometers and 130 micrometers for the AISI 1008 Steel and Magnetic Ingot

Iron, respectively.

2.2 Shock-Loading Procedure

The explosive-loading conditions to permit a correlation of shock hardening and substructure with differences in shock-wave parameters were generated with a computer program.[4] Orava and Wittman[5] introduced the use of the Gurney model for predicting driver-plate velocity from explosive loading. The computer program supplies a rapid means of utilizing these techniques to generate shot specifications from desired parameters. The shot parameters with explosive and tooling dimensions are listed in Table I.

Shock deformation is achieved by the propagation through the material of a planar shock wave produced by means of a "mouse trap" or parallel-plate generator, illustrated in Figure 1. This accelerates a driver plate to a high velocity impact with the specimen assembly shown in Figure 2. This system is designed to prevent spalling and to minimize internal wave reflections and their effects.

The assembly consists of a 1/16-in. (0.16 cm) thick cold-rolled steel cover plate to protect the specimen surface and a 3/4-in. (1.9 cm) thick spall plate. In between the cover plate and spall plate two 3-in. (8.0 cm) by 4-in. (10.0 cm) specimens are placed with the top one being Magnetic Ingot Iron and the lower 1008 Steel. This composite is surrounded by four 1-in. (2.5 cm) thick momentum traps and rests on a 3/4 in. (1.9 cm) thick steel anvil plate. The various components are adhered together by means of an epoxy resin to ensure transmittal of the shock wave across the metal-metal interface. All of the steel used to construct the shot assembly is cold-rolled AISI 1020. The acoustic impedence of AISI 1020 Steel closely matches that of Armco Magnetic Ingot Iron and AISI 1008 Steel.

The driver plate, determined by computer program to generate desired shock-wave parameters, positioned either parallel or inclined to and displaced at the necessary standoff distance from the target, is accelerated by means of an explosive detonated by a plane-wave generator. The plane-wave system, used to detonate this explosive uniformly, is comprised of balsa wood standoffs supporting the driver plate and explosive. The inclined-plate shot setup is used for loads less than 15 GPa. Above 15 GPa the parallel-plate or "mouse trap" assembly is used. In the "mouse trap" assembly, point detonation of the line-wave generator results in the line detonation of the starter charge of Detasheet C-2 placed on the glass plate (Figure 1A). As the two sheets burn, they fracture the glass. The preset angle provides a planar shower of glass fragments onto the main charge. This results in simultaneous detonation over the entire main surface.

The assembly is placed on a piece of insulation board set on a reinforced cardboard box filled with water. The water serves both as a quenching medium and to slow the shot assembly. The steel anvil experiences spallation, but the spall plate/specimen composite is recovered from a pool formed by some of the water originally in the cardboard box.

The explosive used in the experiments is "Detasheet C-1" and "Detasheet C-2," a DuPont PETN-base plastic explosive with density of 1.55×10^2 kg/m^3 and 3.1×10^2 kg/m^3, respectively. The detonation velocity is given by the manufacturer as 7000m sec^{-1}.

The explosive shots were detonated at Ellsworth Air Force Base, Rapid City, South Dakota under the supervision of ordnance officers.

2.3 Hardness Testing Procedure

Measurements were performed on the shot samples immediately upon returning to the lab from the detonation range on an Avery Visual Hardness Testing Machine, Type 6406. The Diamond Pyramid Hardness (DPH) scale was used in this study. The initial readings were made directly on the shot samples at room temperature without surface improvement to provide a near zero-time set of data. After the initial hardness readings were taken, a 1/2-in. (0.013 m) square piece was cut from each 3-in. (0.76 m) by 4-in. (0.102 m) shot sample. These pieces were ambient-temperature mounted in a clear polyester casting resin to enable polishing for better hardness readings during the rest of the room temperature strain aging measurements. The mounted samples, upon curing, were mechanically polished on a Jarrett Precision Polisher to 600 grit. The samples were etched to remove the deformed surface layer. All the remaining shot samples, in order to retain as-shocked properties, were stored at -18°C.

2.4 Metallographic Specimen Preparation

Following the shock-loading process, optical metallographic samples were mounted and ground to 600 grit with silicon carbide paper. The final polish was conducted electrolytically by use of an apparatus shown in Figure 3. The electropolishing was done with a solution containing one part perchloric acid and ten parts glacial acetic acid. The Armco Magnetic Ingot Iron samples required 10V for 3 minutes, and the AISI 1008 Steel required 20V for 4 minutes. The samples were then etched with nital to reveal the grain boundaries.

2.5 Quantitative Metallography

Quantitative metallographic techniques were employed to determine the volume fraction of grains that contained twins, and the volume fraction of

twins within the twinned grains. The point count method was chosen as the most efficient way to measure volume fraction.[6] A 5 by 5 point grid was employed on the metallograph viewing screen. A minimum of 200 grains in area was used for the volume percent of grains containing twins. The point count method was also used to determine the volume percent in each grain.

2.6 Tensile Sample Preparation and Testing

Two tensile samples were cut and machined from each 3-in. (0.076 m) by 4-in. (0.102 m) shot specimen according to ASTM A 370 subsize specimen specifications (Figure 4). Each tensile sample was ground on both faces, exercising care to obtain as near parallel faces as possible. Electropolishing was performed in a solution of one part perchloric acid and ten parts glacial acetic acid at a temperature of 20-25°C. A time of 15 minutes at 30V, with a stainless steel cathode, was required to remove 0.001 inch (0.0025 cm) from the gauge thickness.

All tensile specimens were tested at room temperature on an MTS testing machine (Model No. 914.69). The specimens were loaded at a nominal strain rate of 10^{-3} sec^{-1}. Following failure, the cross-sectional area was measured by micrometer to determine reduction in area. The 0.2% offset yield, ultimate tensile strength (UTS), and % uniform elongation to UTS were then determined from the graphical MTS output.

III. Experimental Results

3.1 Optical Metallography

The microstructures of the shock-loaded Armco Magnetic Ingot Iron and the AISI 1008 Steel both exhibited twinning as the predominant feature. An X-ray diffractometer analysis of the as-shocked specimens revealed the presence of only B.C.C. alpha iron, with no detectable amount of high-pressure

epsilon being retained upon unloading.

With duration and rarefaction rate held constant, a variation of peak pressure has a significant effect on the percentage of grains which contain twins after shock loading. The photomicrographs shown in Figures 5 and 6 show that as peak pressure increases the number of grains containing twins plus the volume fraction within twinned grains increases.

Increased peak pressure duration increases the volume fraction of grains exhibiting twins and the number of twins within twinned grains in shock-loaded iron and steel. This result is shown in Figures 7 and 8. Shot pairs where rarefaction rate and pressure are held constant, such as shots 10 and 11, shots 13 and 14, and shots 16 and 17, in particular, show that increased duration increases twin volume fraction. Twin formation in both the materials studied are more influenced by duration between 0.5 and 1.0 μsec than between 1.0 and 2.0 μsec. These data are presented in Table II.

The remaining shock-wave parameter, rarefaction rate, was found to have a less pronounced effect on the shocked microstructure. Figures 9 and 10 both demonstrate that at a given pressure and duration the higher rarefaction rate favors smaller twins than does a lower rarefaction rate. The effect of rarefaction rate on volume fraction of twins formed is not well pronounced. No systematic trend across all shock pressures was detected. All data related to the role of rarefaction rate are tabulated in Table III.

3.2 Hardness and Room Temperature Strain Aging

When duration and rarefaction are held constant a moderate increase in hardness on the Diamond Pyramid Hardness scale (DPH), was observed for the 8, 10, and 13 GPa pressures. Between 13 and 25 GPa pressure, the

hardness jumped more than 100 DPH points for both materials studied. The data showing these results are plotted along with the data of Zukas[2] and Dieter[3] in Figure 11.

Strain aging at room temperature is occurring in the Armco Ingot Iron and 1008 Steel between the time of the explosive event and 48 hours. After 48 hours, no significant change in hardness with time was observed. These results are provided in Figures 12 and 13. The absence of data points in Figures 12 and 13 at 3 to 4 hours after shock loading for several of the tests, is related to the poor condition of the specimen surface, making usable hardness measurement impossible.

When duration is varied with peak pressure and rarefaction rate held constant, a direct correlation is also observed between hardness and microstructure. The hardness data tabulated in Table IV for shot pairs 10 and 11, and 13 and 14, could be compared with the photomicrographs in Figures 7 and 8. It appears that in the pressure range of 13 to 33 GPa, where three waves would traverse the iron specimens, duration is significant in developing the microstructure and mechanical properties of the material. Duration appears to have had little or no effect on microstructure or hardness between 8-13 GPa and above 33 GPa pressure. A summary of some of the hardness data are given in Table IV.

When peak pressure and pressure duration are held constant, it appears that varying rarefaction rate results in no systematic modification of microstructure or hardness, with one exception -- shot pair 11 and 12. Table V provides a summary of DPH hardness data to show the role of rarefaction rate.

3.3 Tensile Properties

Peak pressure is seen to affect the yield strength and ultimate tensile strength (UTS) significantly (Figure 14, A and B). The engineering stress-

strain curves with only peak pressure changing demonstrate the marked increase in strength for the 25 and 35 GPa shots over the lower pressure shots. All the stress-strain curves fail to show the typical work-hardening behavior of ordinary steels. Instead, the stress-strain curves show signs of early plastic instability such that the UTS is reached at small tensile elongations. These results are shown in Figures 15 and 16.

The amount of elongation to UTS present for material shocked at or below 13 GPa is similar. The 25 and 35 GPa shots yielded greatly reduced elongations to UTS. The presence of a plastic instability is further exemplified by the data on percent elongation to UTS and for reduction in area. When the materials are shocked to higher pressures, a very low elongation to UTS is observed with considerable reduction in area still present. (See Tables VI and VII).

Increased pulse duration is observed to increase the 0.2% offset yield of both materials (Table VIII). Figures 17 and 18 show that increased duration increases yield strength, especially after the 25 and 35 GPa shots.

The amount of reduction in area is slightly lower in the higher duration shots. Uniform elongation to UTS is also slightly affected with the higher duration shots exhibiting increased elongations prior to failure. These trends are shown in Figures 17 and 18.

Rarefaction rate is found to be the least significant shock parameter. Little systematic trend was detectable in the dependence of tensile behavior on rarefaction rate. Out of a total of 24 strength comparisons, (yield and UTS), in 14 cases the higher strength was associated with a lower rarefaction rate. In comparing ductility, 9 of the 24 had a lower ductility associated with a lower rarefaction rate.

IV. Tentative Conclusions

A detailed discussion of the results will not be presented until all of the electron microscopy is completed. However, several significant tentative conclusions can be listed.

1) Peak pressure is the most significant shock-strengthening parameter. An increase in peak pressure increases the tensile strength and hardness.

2) For material shocked between 25 GPa and 35 GPa pressure, a two-fold increase in UTS is observed. Residual hardness increases between 13 GPa and 25 GPa and appears to level off.

3) A variation in pulse duration does contribute to minor differences in the shock strengthening of iron. The volume fraction of twins was shown to increase with increased duration. Increasing the pulse duration also leads to increase the 0.2% offset yield. The effects of duration were found to be more pronounced in the 13-33 GPa pressure range.

4) Rarefaction rate is found to be the least significant shock parameter. No systematic modification in mechanical properties or microstructure was observed. Accordingly, in previous work, pulse duration effects can probably be attributed to duration and not to concurrent changes in rarefaction rate.

V. Expected Progress (July 1, 1977 through December 31, 1977)

Major progress will be made in completing the substructure characterization by means of electron microscopy. The thermal recovery part of the program is currently progressing well, and the experimental part of this study should be completed by the end of December.

References

1. G. A. Stone and R. N. Orava, "The Influence of Shock-Wave Parameters on the Shock Strengthening of Nickel," to be submitted for publication, South Dakota School of Mines and Technology, Rapid City, SD 57701.

2. E. G. Zukas, "Shock Wave Strengthening" Metals Engineering Quarterly, Vol. 6, p. 1-20, May, 1966.

3. G. E. Dieter, Strengthening Mechanisms in Solids, ASM, Metals Park, Ohio, p. 279-340, 1962.

4. R. O. Lokken, "An Investigation of the Influence of Shock-Wave Parameters on the Shock Strengthening of Nickel," MS Thesis, South Dakota School of Mines and Technology, Rapid City, SD (1976).

5. R. N. Orava and R. H. Wittman, "Techniques for the Control and Application of Explosive Shock Waves," Proc. 5th Intl. Conf. on High Energy Rate Fabrication held in June, 1975.

6. E. E. Underwood, "Applications of Quantitative Metallography," ASM Metals Handbook, Vol. 8, 8th ed., p. 39, 1973.

TABLE I
PARAMETRIC, TOOLING, AND EXPLOSIVE REQUIREMENTS
FOR 18 SHOCK-LOADING EXPERIMENTS

SHOT #	PEAK PRESSURE (GPa)	PRESSURE DURATION (μsec)	RAREFACTION RATE (GPa/μsec)	DRIVER PLATE	DRIVER VELOCITY (m/sec)	DRIVER THICKNESS (mm)	EXPLOSIVE NEEDED (# sheets) C1	C2
1	8.0	1.0	-51.55	nickel	437.23	2.674	0	2
2	8.0	1.0	-34.90	1018-ST	502.92	1.925	1	1
3	8.0	2.0	-35.00	304-SS	459.14	4.970	1	3
4	10.0	1.0	-51.40	304-SS	562.20	2.793	1	2
5	10.0	1.0	-36.50	1018-ST	612.71	2.531	1	2
6	10.0	2.0	-36.40	304-SS	562.20	5.028	1	4
7	13.0	1.0	-51.00	copper	713.07	2.577	1	3
8	13.0	1.0	-38.80	1018-ST	768.81	2.282	0	3
9	13.0	2.0	-38.50	304-SS	710.15	5.441	1	6

TABLE I CONT.
PARAMETRIC, TOOLING, AND EXPLOSIVE REQUIREMENTS
FOR 18 SHOCK-LOADING EXPERIMENTS

SHOT #	PEAK PRESSURE (GPa)	PRESSURE DURATION (μsec)	RAREFACTION RATE (GPa/μsec)	DRIVER PLATE	DRIVER VELOCITY (m/sec)	DRIVER THICKNESS (mm)	EXPLOSIVE NEEDED (# sheets) C1	C2
10	18.0	0.5	-63.80	2024-AL	1479.40	1.926	1	1
11	18.0	1.0	-63.30	nickel	898.46	2.766	1	3
12	18.0	1.0	-42.50	1018-ST	1010.18	2.693	1	3
13	25.0	0.5	-71.80	2024-AL	1934.38	2.105	1	2
14	25.0	1.0	-70.50	nickel	1185.18	3.031	1	5
15	25.0	1.0	-51.10	2024-AL	1934.38	4.211	0	5
16	35.0	0.5	-78.00	921T-AL	2522.91	2.524	0	5
17	35.0	1.0	-79.90	nickel	1558.49	3.356	0	9
18	35.0	1.0	-53.30	1018-ST	1710.78	3.286	0	9

TABLE II
EFFECT OF PULSE DURATION ON THE VOLUME FRACTION OF TWINNED GRAINS AND % VOLUME OF TWINS WITHIN GRAINS

SHOT	PEAK PRESSURE (GPa)	PRESSURE DURATION (μsec)	RAREFACTION RATE (GPa/μsec)	VOLUME % OF GRAINS WITH TWINS		VOLUME % TWINS WITHIN TWINNED GRAINS	
				MAG FE	1008	MAG FE	1008
2	8.0	1.0	-34.90	3	0	20	0
3	8.0	2.0	-35.00	2	2	15	7
5	10.0	1.0	-36.50	10	5	75	10
6	10.0	2.0	-36.40	12	5	77	5
8	13.0	1.0	-38.80	55	12	22	8
9	13.0	2.0	-38.50	42	21	25	53
10	18.0	0.5	-63.80	31	10	12	30
11	18.0	1.0	-63.30	61	32	75	9
13	25.0	0.5	-71.80	5	2	11	3
14	25.0	1.0	-70.50	42	60	68	10
16	35.0	0.5	-78.00	73	45	85	46
17	35.0	1.0	-79.90	77	87	95	96

TABLE III
EFFECT OF RAREFACTION RATE ON THE VOLUME FRACTION OF TWINNED GRAINS AND % VOLUME OF TWINS WITHIN GRAINS

SHOT	PEAK PRESSURE (GPa)	PRESSURE DURATION (μsec)	RAREFACTION RATE (GPa/μsec)	VOLUME % OF GRAINS WITH TWINS		VOLUME % TWINS WITHIN TWINNED GRAINS	
				MAG FE	1008	MAG FE	1008
1	8.0	1.0	-51.55	0	0	0	0
2	8.0	1.0	-34.90	3	0	20	0
4	10.0	1.0	-51.40	1	8	17	28
5	10.0	1.0	-36.50	10	5	75	10
7	13.0	1.0	-51.00	13	15	63	10
8	13.0	1.0	-38.80	55	12	22	8
11	18.0	1.0	-63.30	61	32	75	9
12	18.0	1.0	-42.50	61	76	12	10
14	25.0	1.0	-70.50	42	60	68	10
15	25.0	1.0	-51.10	57	66	62	57
17	35.0	1.0	-79.90	77	87	95	96
18	35.0	1.0	-53.30	62	88	84	95

TABLE IV
EFFECT OF PULSE DURATION ON THE ROOM TEMPERATURE
STRAIN AGING OF MAGNETIC INGOT IRON AND AISI 1008

SHOT	PEAK PRESSURE (GPa)	PRESSURE DURATION (μsec)	RAREFACTION RATE (GPa/μsec)	DPH			
				MAG FE		1008	
				2 DAYS AFTER SHOT	24 DAYS AFTER SHOT	2 DAYS AFTER SHOT	24 DAYS AFTER SHOT
2	8.0	1.0	-34.90	116±3	112±2	129±5	137±4
3	8.0	2.0	-35.00	109±3	106±2	121±3	131±4
5	10.0	1.0	-36.50	125±4	123±4	126±4	132±2
6	10.0	2.0	-36.40	122±1	120±2	124±2	127±4
8	13.0	1.0	-38.80	145±8	154±4	130±4	137±3
9	13.0	2.0	-38.50	120±4	125±3	144±4	147±5
10	18.0	0.5	-63.80	125±2	129±9	138±7	136±2
11	18.0	1.0	-63.30	195±6	188±6	234±9	213±24
13	25.0	0.5	-71.80	119±2	124±4	126±6	132±4
14	25.0	1.0	-70.50	230±11	256±10	248±12	251±30
16	35.0	0.5	-78.00	239±8	263±8	251±7	270±6
17	35.0	1.0	-79.90	237±8	246±10	262±7	275±6

TABLE V
EFFECT OF RAREFACTION RATE ON THE ROOM TEMPERATURE
STRAIN AGING OF MAGNETIC INGOT IRON AND AISI 1008

SHOT	PEAK PRESSURE (GPa)	PRESSURE DURATION (μsec)	RAREFACTION RATE (GPa/μsec)	DPH			
				MAG FE		1008	
				2 DAYS AFTER SHOT	24 DAYS AFTER SHOT	2 DAYS AFTER SHOT	24 DAYS AFTER SHOT
1	8.0	1.0	-51.55	109±4	106±3	122±2	127±2
2	8.0	1.0	-34.90	116±3	112±2	129±5	137±4
4	10.0	1.0	-51.40	120±3	124±3	131±7	131±5
5	10.0	1.0	-36.50	125±4	123±4	126±4	132±2
7	13.0	1.0	-51.00	130±3	124±4	138±4	146±5
8	13.0	1.0	-38.80	145±8	154±4	130±4	137±3
11	18.0	1.0	-63.30	195±6	188±6	234±9	213±24
12	18.0	1.0	-42.50	159±3	168±10	142±14	146±8
14	25.0	1.0	-70.50	230±11	256±10	248±12	251±30
15	25.0	1.0	-51.10	242±10	262±6	248±10	262±4
17	35.0	1.0	-79.90	237±8	246±10	242±7	275±6
18	35.0	1.0	-53.30	214±7	220±1	233±5	246±7

TABLE VI

TENSILE PROPERTIES OF MAGNETIC INGOT IRON

SHOT	UTS (MN/m^2)	% ELONGATION TO UTS	% REDUCTION IN AREA
–	285.8	26.6	81.52
1	295.2	11.5	79.08
2	296.2	17.5	73.18
3	280.8	26.9	80.56
4	301.1	12.3	77.95
5	288.8	23.1	81.37
6	292.0	14.8	82.24
7	303.7	13.2	76.28
8	339.0	7.4	80.81
9	298.6	21.5	77.04
10	306.0	6.5	77.36
11	421.6	1.5	68.67
12	392.0	3.2	71.56
13	327.0	0.45	79.16
14	328.6	6.25	73.60
15	629.0	1.5	60.58
16	494.4	1.0	72.60
17	618.5	2.1	59.94
18	593.9	1.7	54.02

TABLE VII

TENSILE PROPERTIES OF AISI 1008 STEEL

SHOT	UTS (MN/m^2)	% ELONGATION TO UTS	% REDUCTION IN AREA
-	305.6	24.4	74.67
1	318.8	12.4	69.52
2	326.2	11.9	66.92
3	360.9	19.5	67.80
4	330.7	18.3	74.02
5	348.0	6.6	68.99
6	334.0	15.3	65.86
7	345.0	3.6	68.93
8	326.5	13.8	74.35
9	325.1	25.7	75.61
10	351.0	28.4	69.76
11	361.9	11.0	67.75
12	367.9	4.3	69.65
13	340.4	25.1	70.39
14	347.6	7.9	72.90
15	680.6	5.8	44.45
16	559.2	1.4	57.08
17	705.1	5.6	53.98
18	718.8	5.6	52.05

TABLE VIII
YIELD STRENGTH 0.2 % OFFSET DATA FOR
MAGNETIC INGOT IRON AND AISI 1008 STEEL

SHOT	PRESSURE (GPa)	DURATION (μsec)	RAREFACTION RATE (GPa/μsec)	YIELD STRENGTH (MN/m^2) MAG FE	1008
-	-	-	-	125.4	210.2
1	8.0	1.0	-51.5	292.5	265.0
2	8.0	1.0	-34.9	291.3	311.5
3	8.0	2.0	-35.0	214.5	297.4
4	10.0	1.0	-51.4	294.0	309.4
5	10.0	1.0	-36.5	261.9	304.9
6	10.0	2.0	-36.4	272.1	323.8
7	13.0	1.0	-51.0	279.1	325.4
8	13.0	1.0	-38.8	324.7	307.0
9	13.0	2.0	-38.5	284.8	307.4
10	18.0	0.5	-63.8	296.2	291.5
11	18.0	1.0	-63.3	318.3	306.9
12	18.0	1.0	-42.5	338.8	338.3
13	25.0	0.5	-71.8	319.6	304.4
14	25.0	1.0	-70.5	328.6	329.2
15	25.0	1.0	-51.1	433.1	364.7
16	35.0	0.5	-78.0	399.6	407.2
17	35.0	1.0	-79.9	424.5	478.4
18	35.0	1.0	-53.3	475.3	420.8

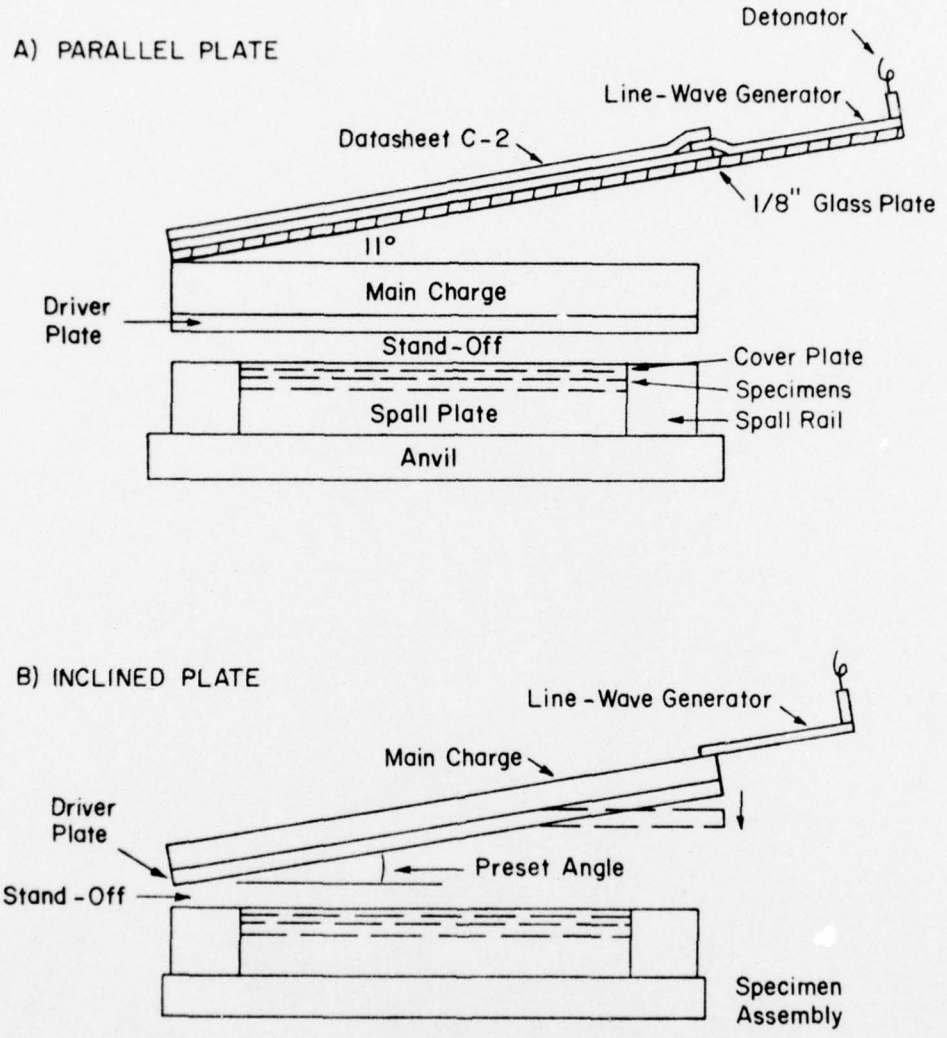

Figure 1. Plate Impact Plane-Wave Generators

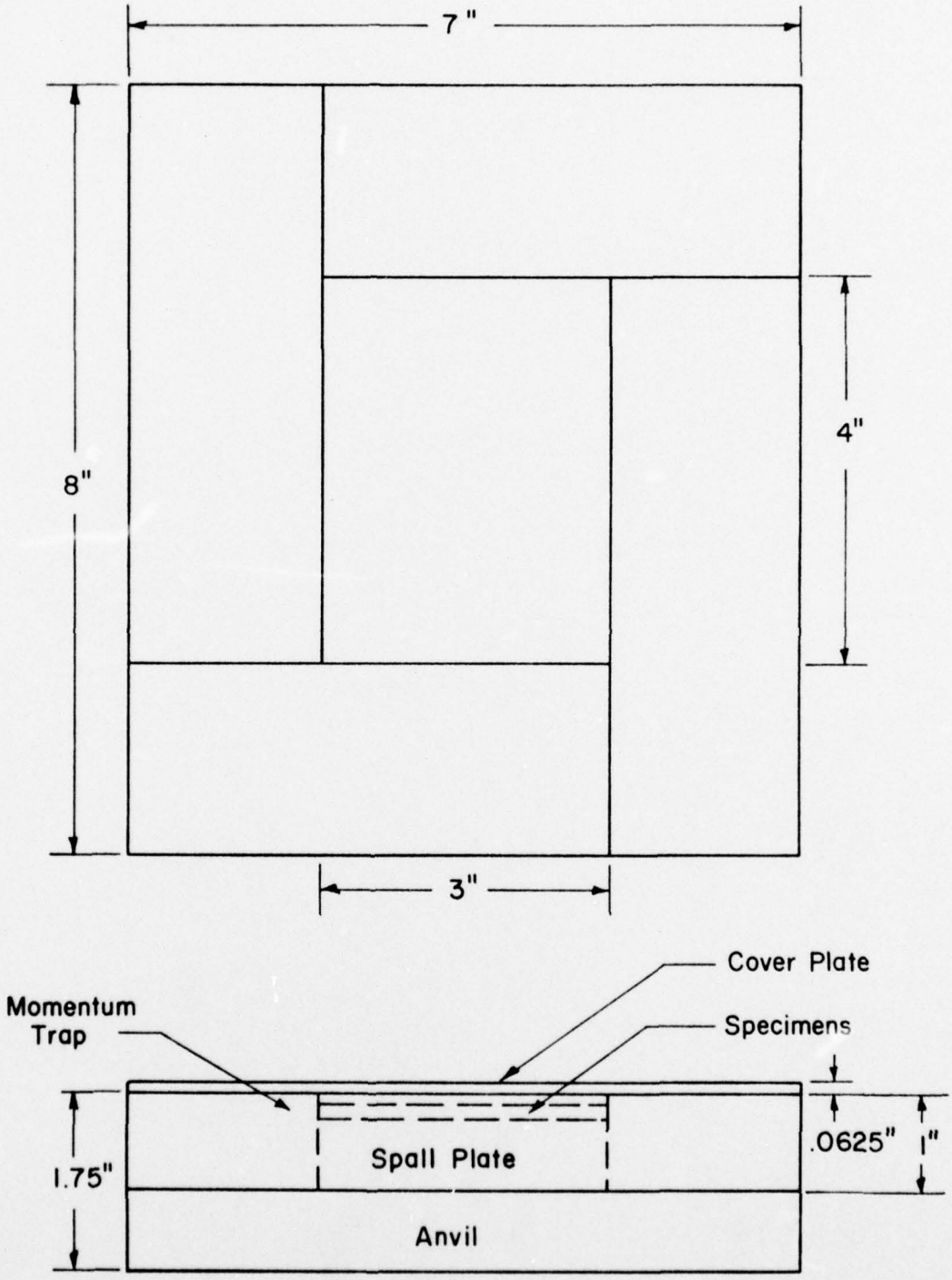

Figure 2. Specimen Assembly

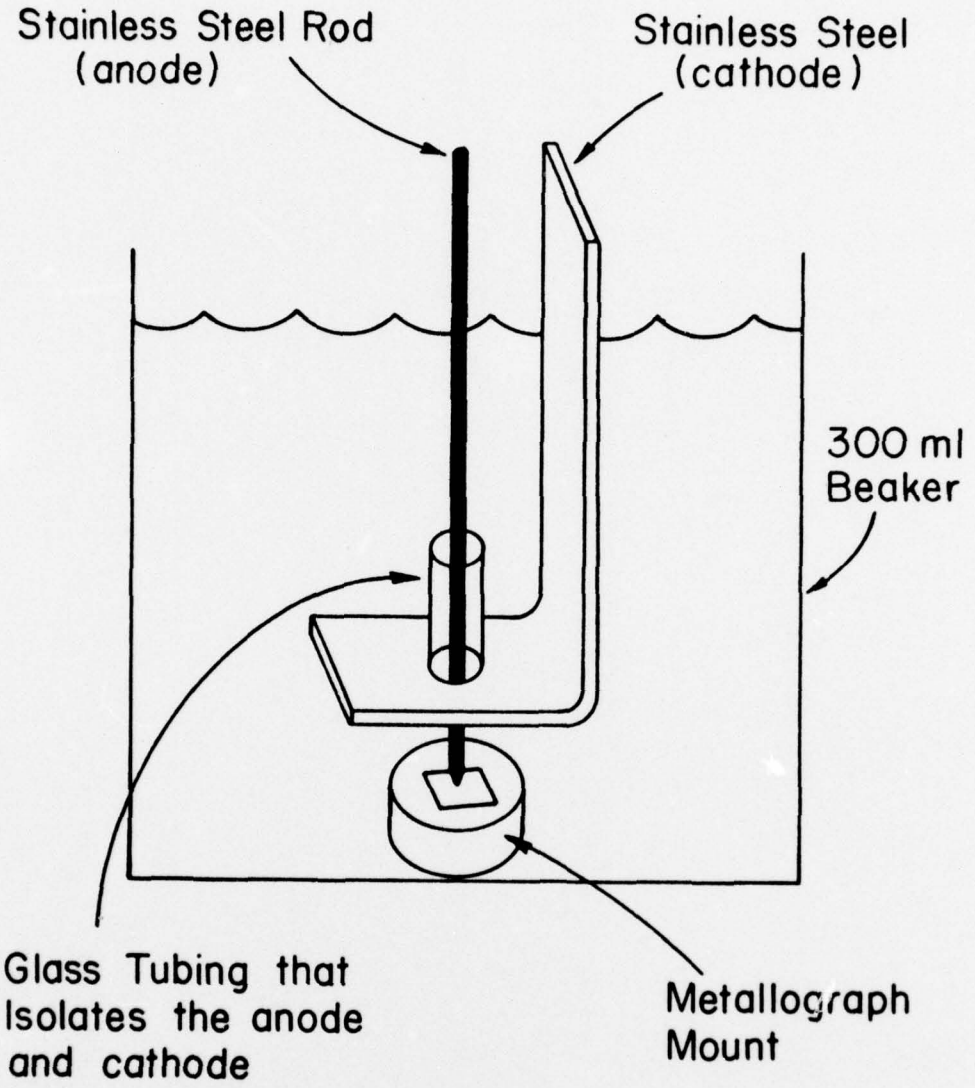

Figure 3. Electropolishing Apparatus for Optical Metallographic Sample Preparation

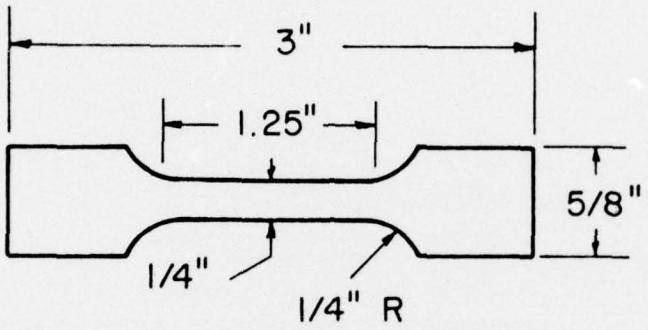

ASTM A 370 SUBSIZE SPECIMEN

Figure 4. Tensile Specimen

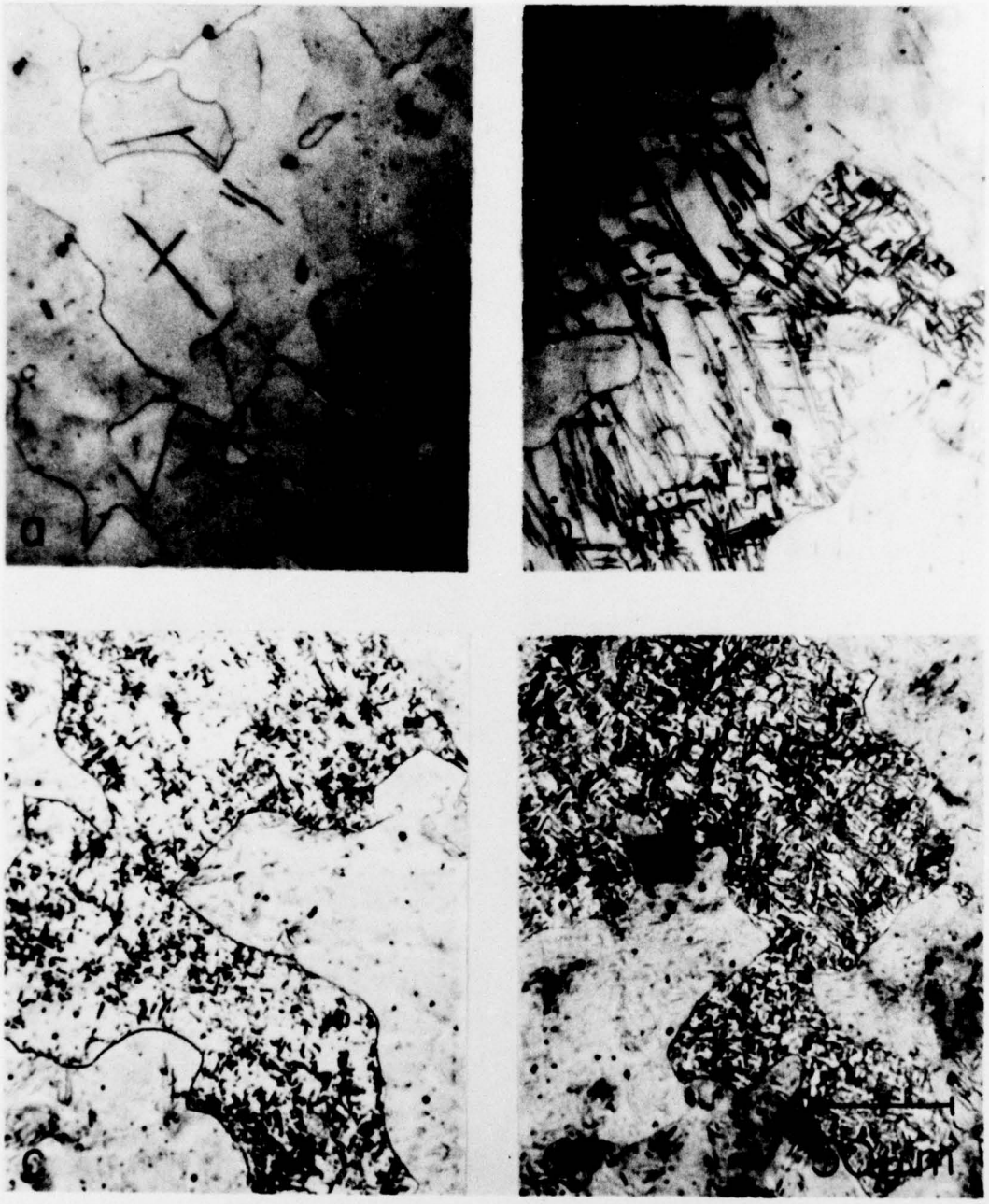

Figure 5. Microstructure of Shock-Hardened Armco Magnetic Ingot Iron as a Function of Shock Pressure at Constant Pressure Duration and Rarefaction Rate: (a) 10 GPa, (b) 13 GPa, (c) 25 GPa, (d) 35 GPa.

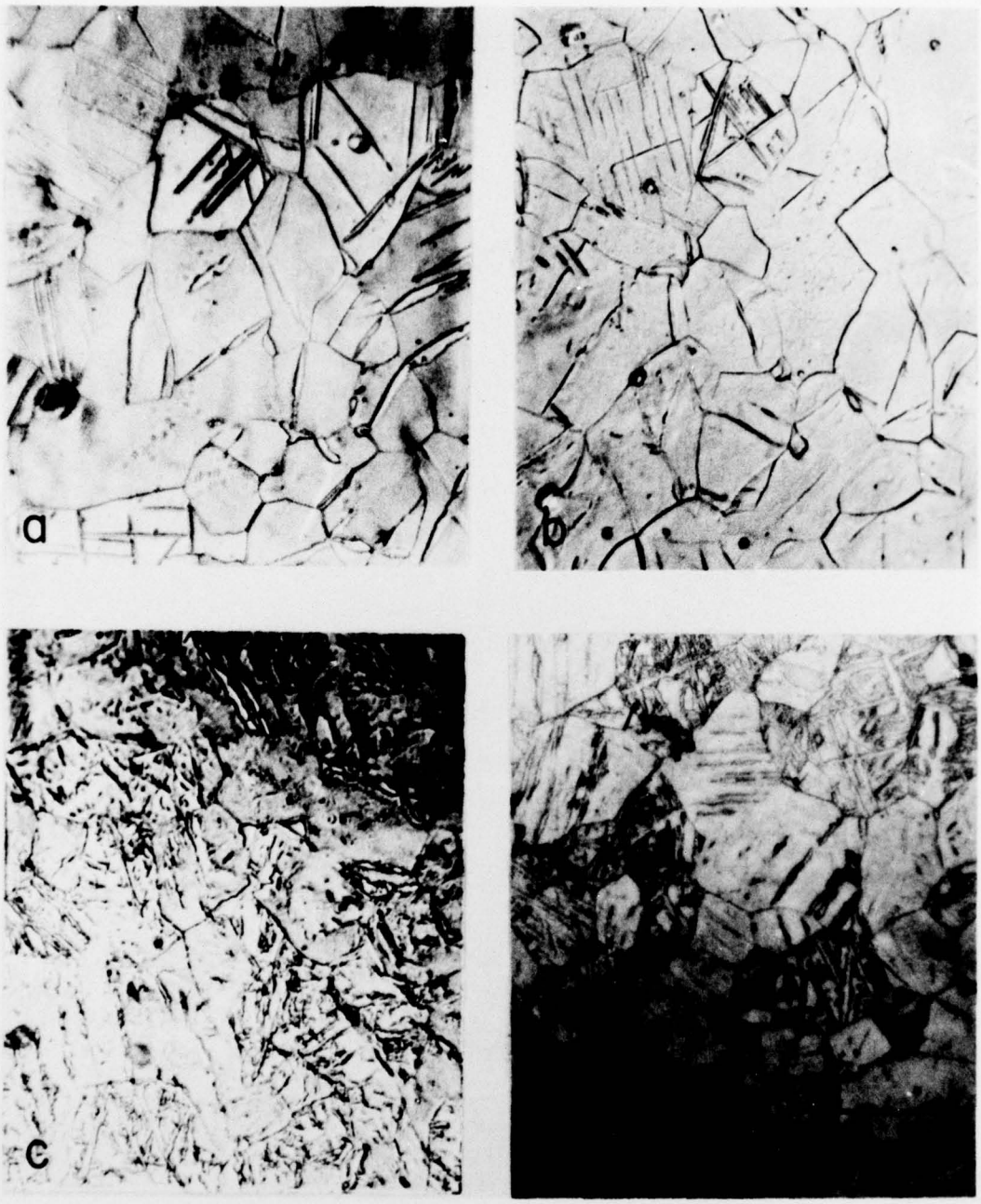

Figure 6. Microstructure of Shock-Hardened AISI 1008 Steel as a Function of Shock Pressure at Constant Pressure Duration and Rarefaction Rate (a) 10 GPa, (b) 13 GPa, (c) 25 GPa, (d) 35 GPa.

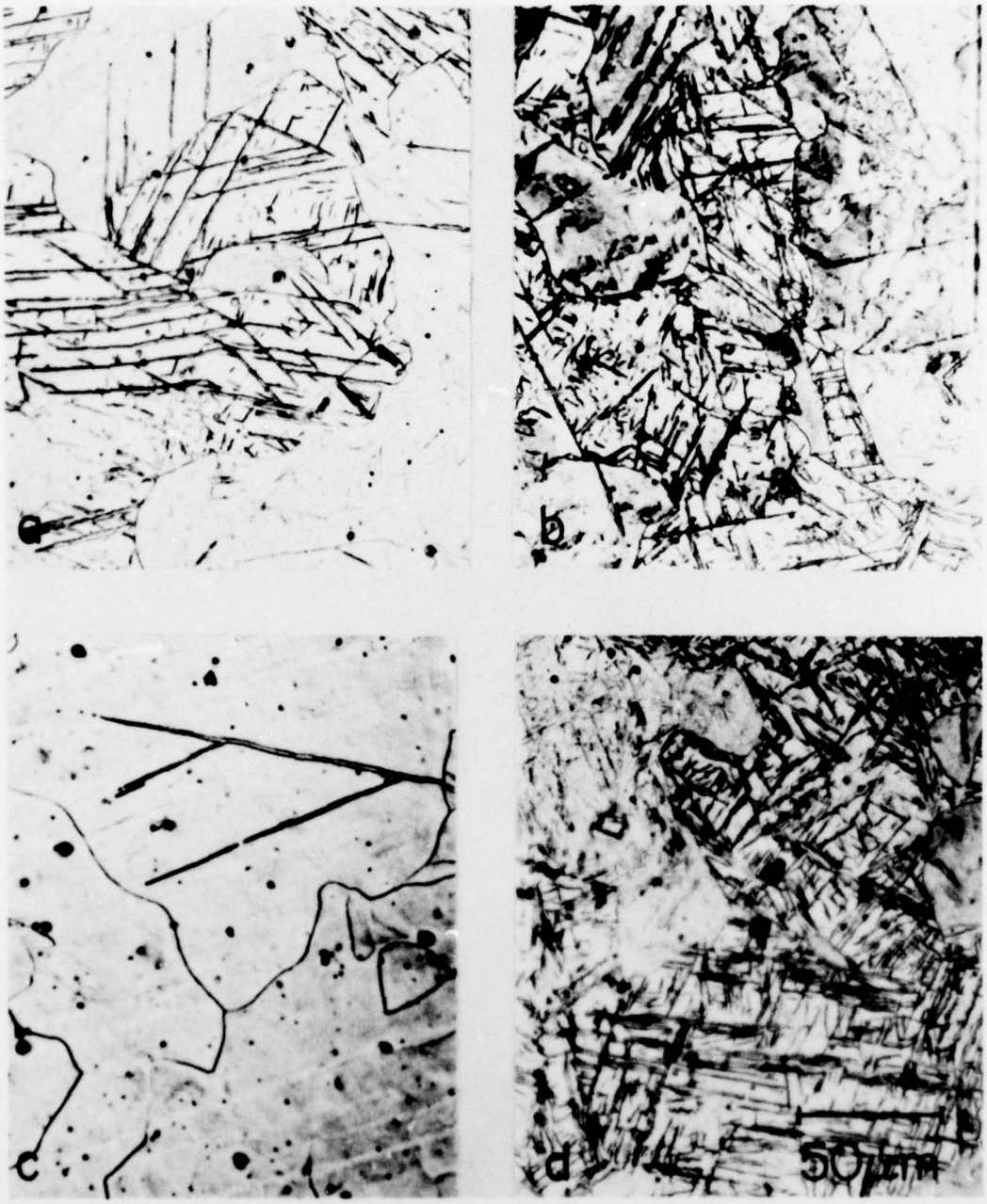

Figure 7. Microstructure of Shock-Hardened Armco Magnetic Ingot Iron as a Function of Peak Pressure Duration. (a) 18 GPa pressure, -63.8 GPa/μsec rarefaction, 0.5 μsec duration, (b) same as (a) except 1.0 μsec duration, (c) 25 GPa pressure, -71.0 GPa/μsec rarefaction, 0.5 μsec duration, (d) same as (c) except 1.0 μsec duration.

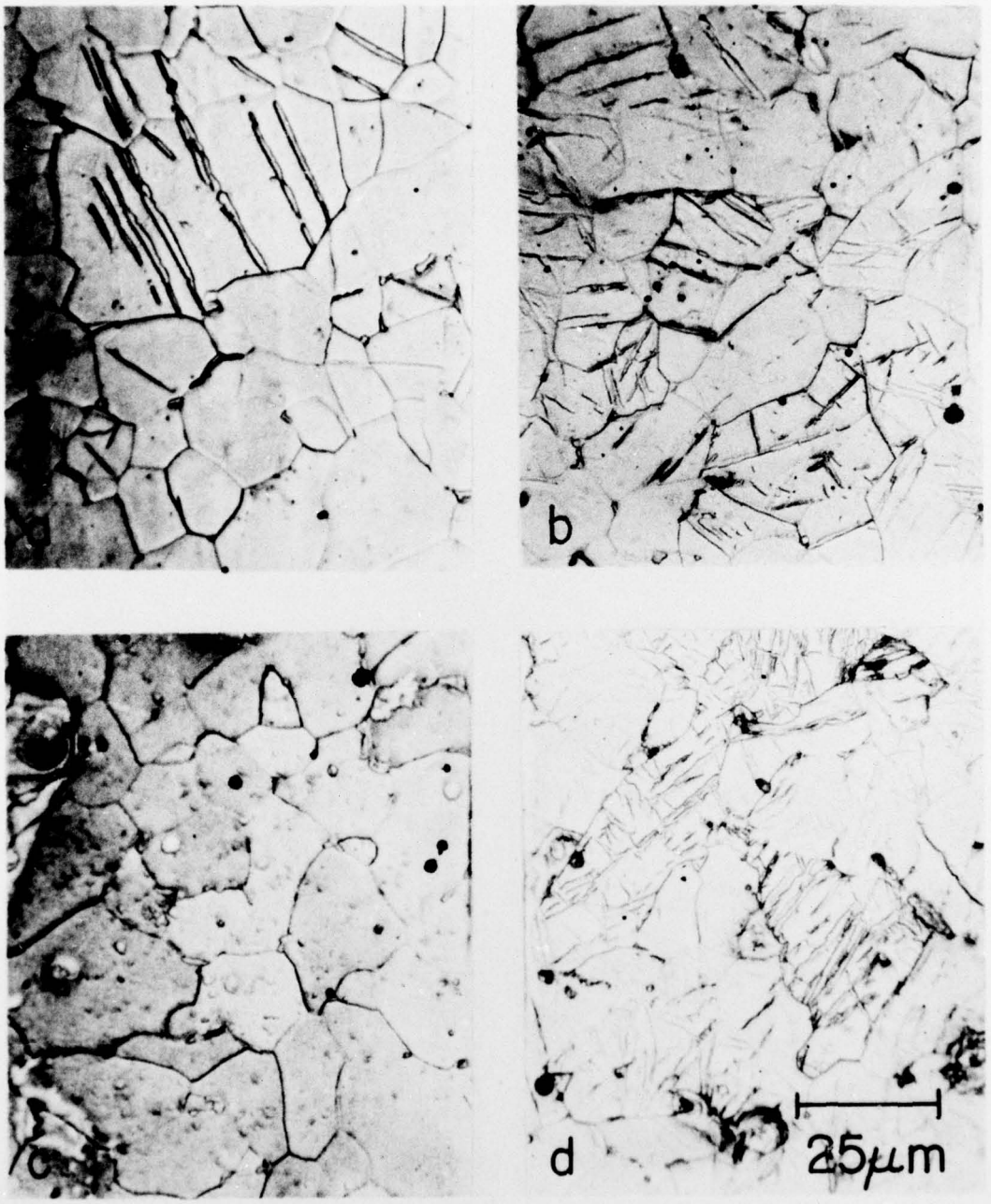

Figure 8. Microstructure of Shock-Hardened AISI 1008 Steel as a Function of Peak Pressure Duration. (a) 18 GPa pressure,-63.8 GPa/μsec rarefaction, 0.5 μsec duration, (b) same as (a) except 1.0 μsec duration, (c) 25 GPa pressure,-71.0 GPa/μsec rarefaction, 0.5 μsec duration, (d) same as (c) except 1.0 μsec duration.

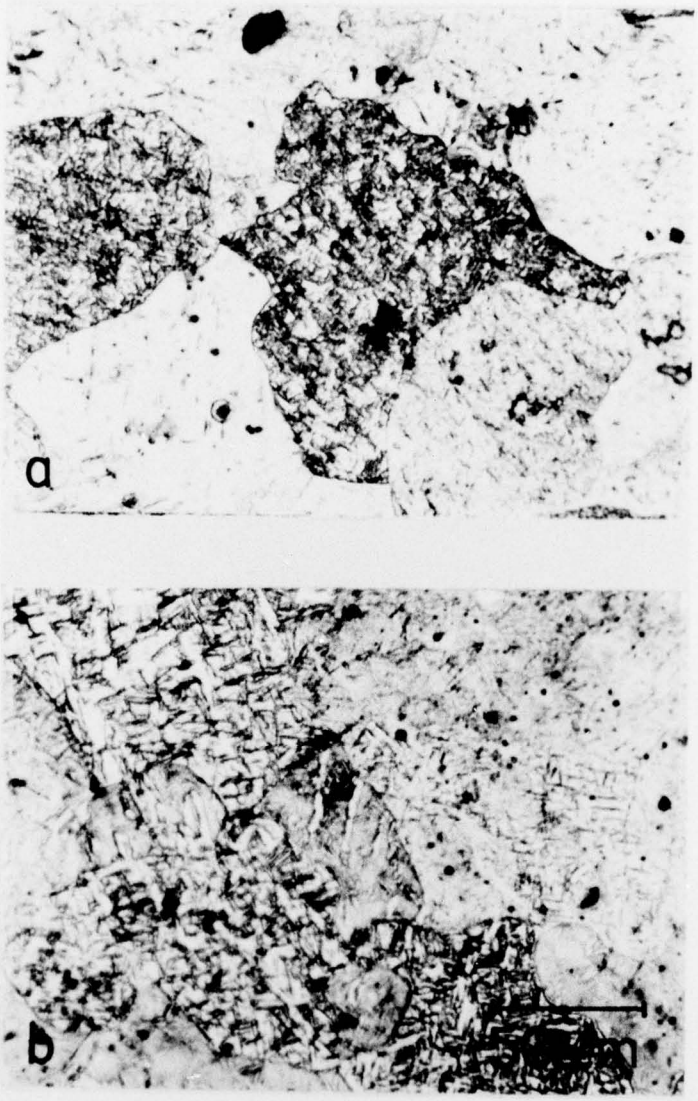

Figure 9. Microstructure of Shock-Hardened Armco Magnetic Ingot Iron as a Function of Rarefaction Rate. (a) 35 GPa pressure, 1.0 μsec duration, -79.9 GPa/μsec rarefaction rate, (b) same as (a) except -53.3 GPa/μsec rarefaction rate.

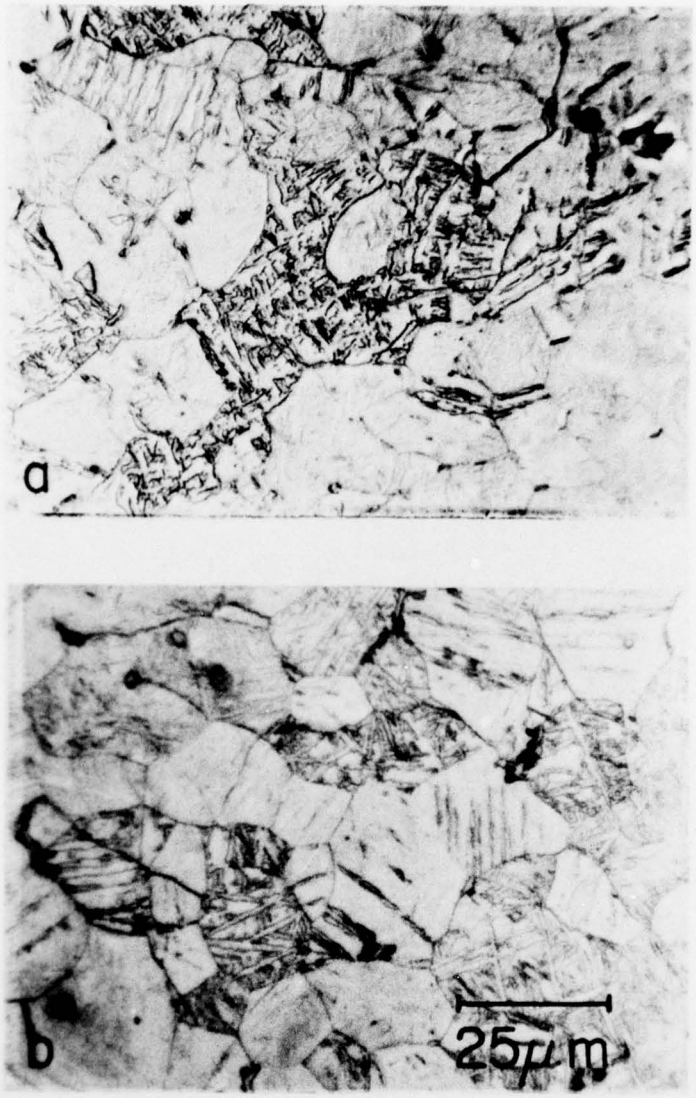

Figure 10. Microstructure of Shock-Hardened AISI 1008 Steel as a Function of Rarefaction Rate. (a) 35 GPa pressure, 1.0 μsec duration, -79.9 GPa/μsec rarefaction rate, (b) same as (a) except -53.3 GPa/μsec rarefaction rate.

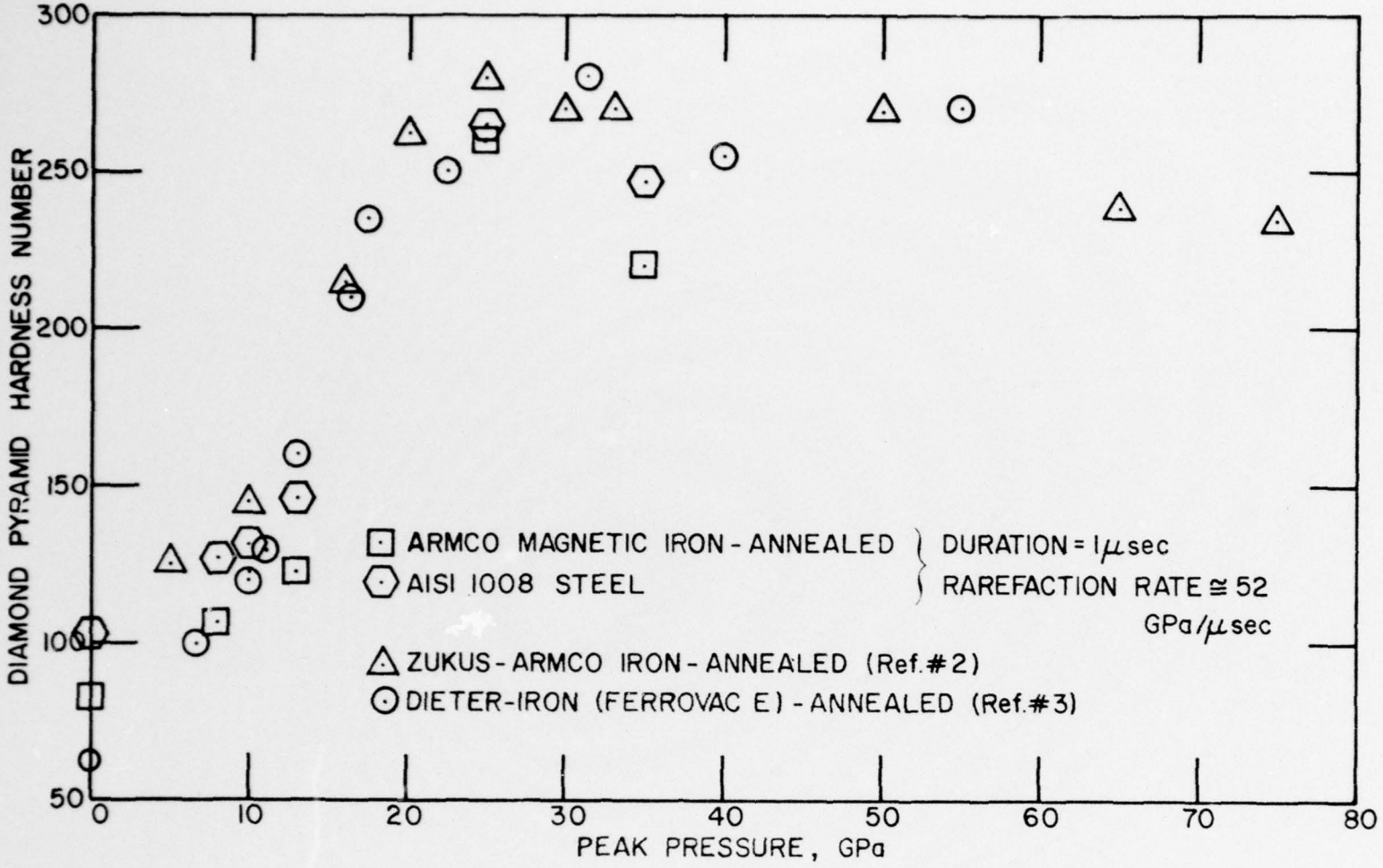

Figure 11. Available Data Showing DPH Hardness vs. Peak Pressure for Iron and Steel.

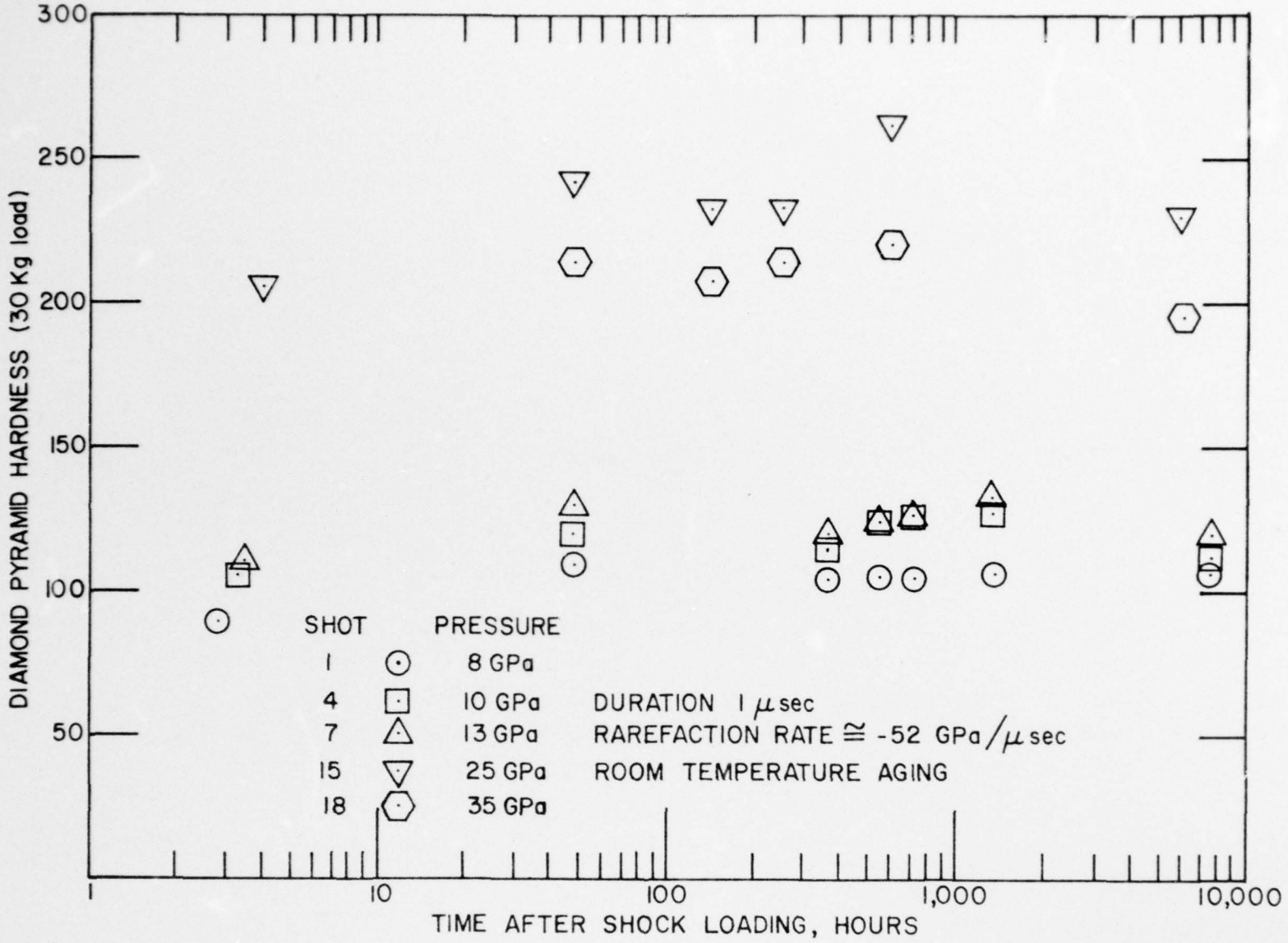

Figure 12. Room Temperature Aging of Armco Magnetic Ingot Iron.

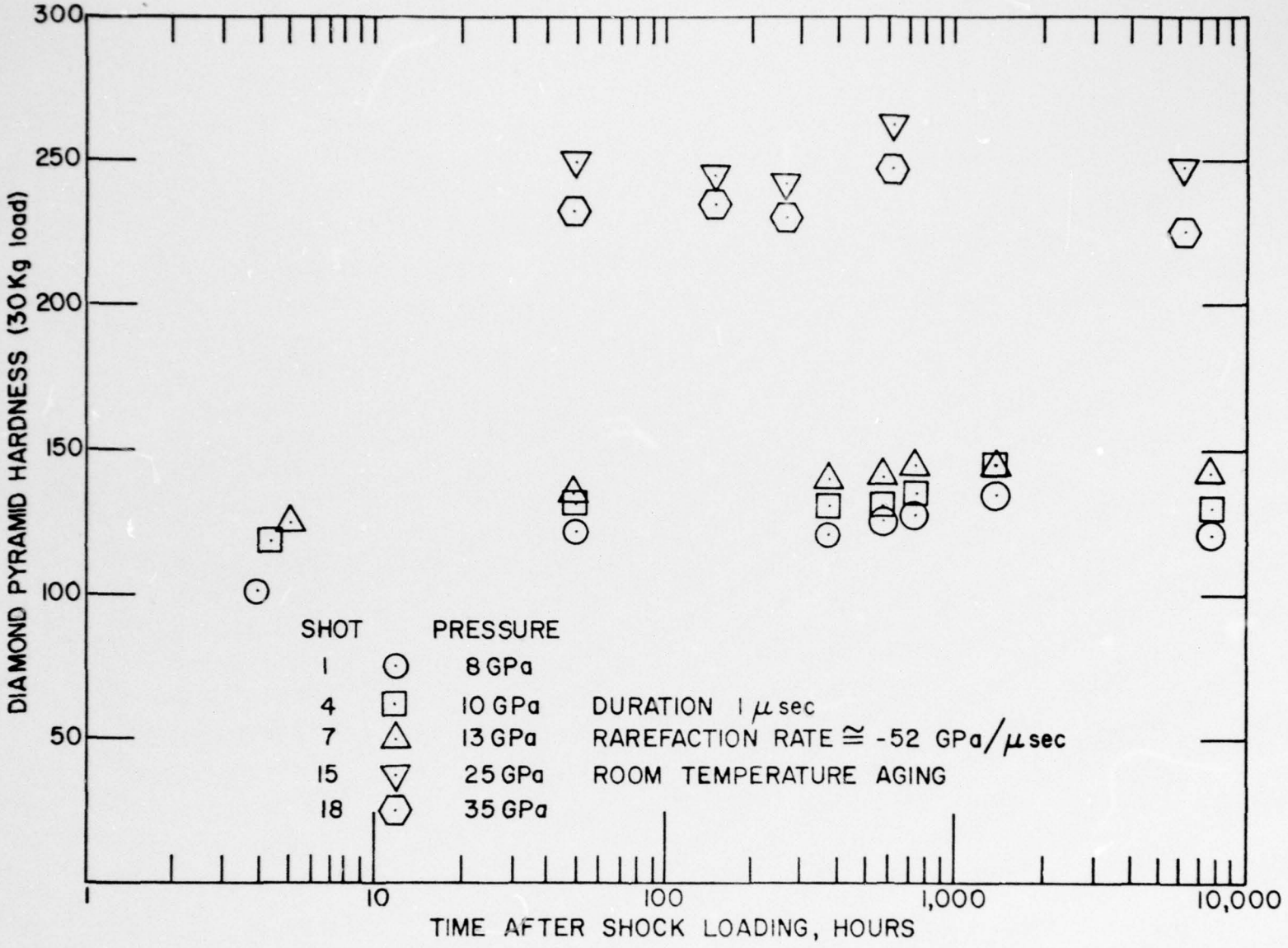

Figure 13. Room Temperature Aging of AISI 1008 Steel.

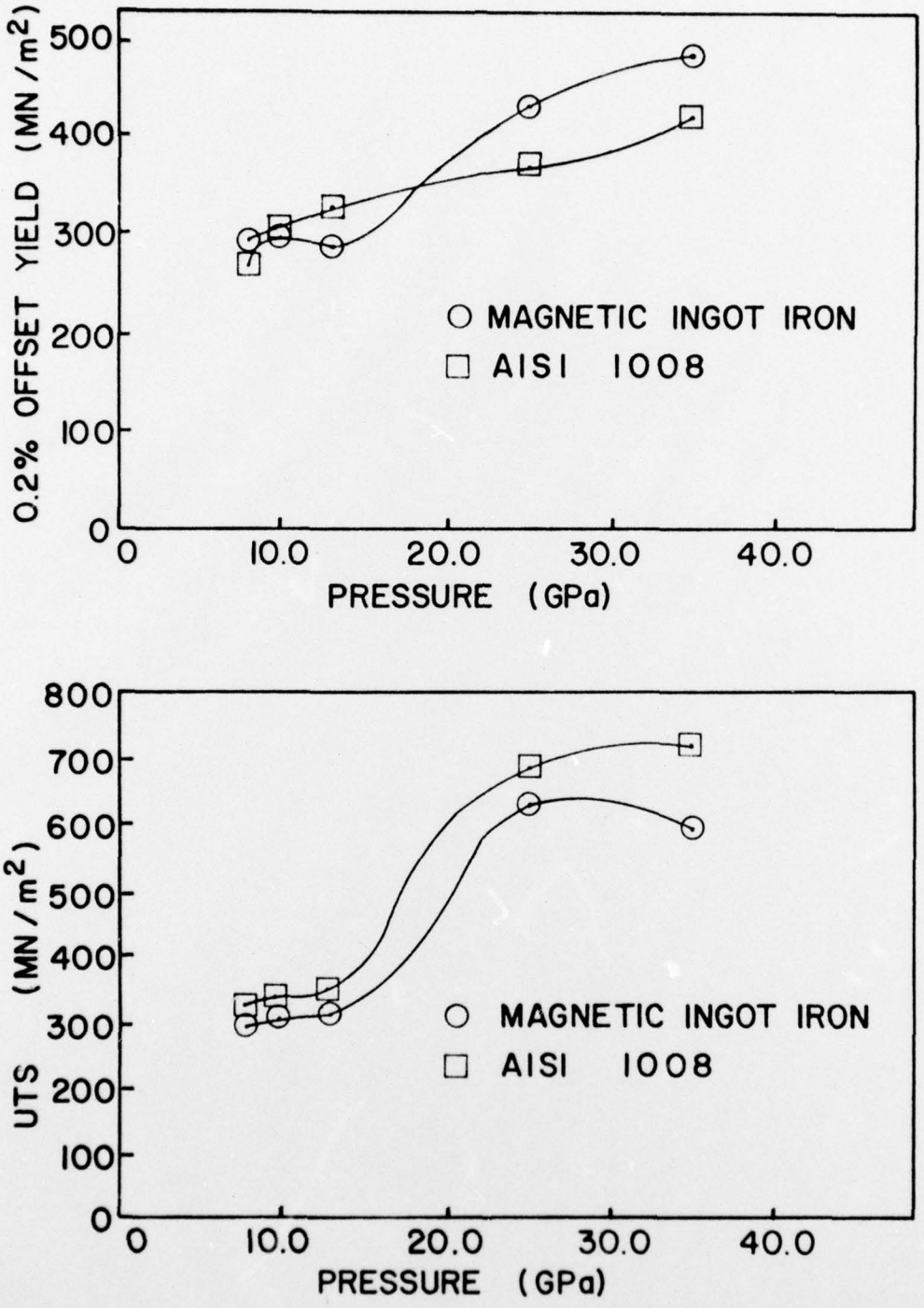

Figure 14. The Effect of Peak Pressure on the (a) 0.2% Offset Yield, (b) UTS, with Constant Duration and Rarefaction Rate.

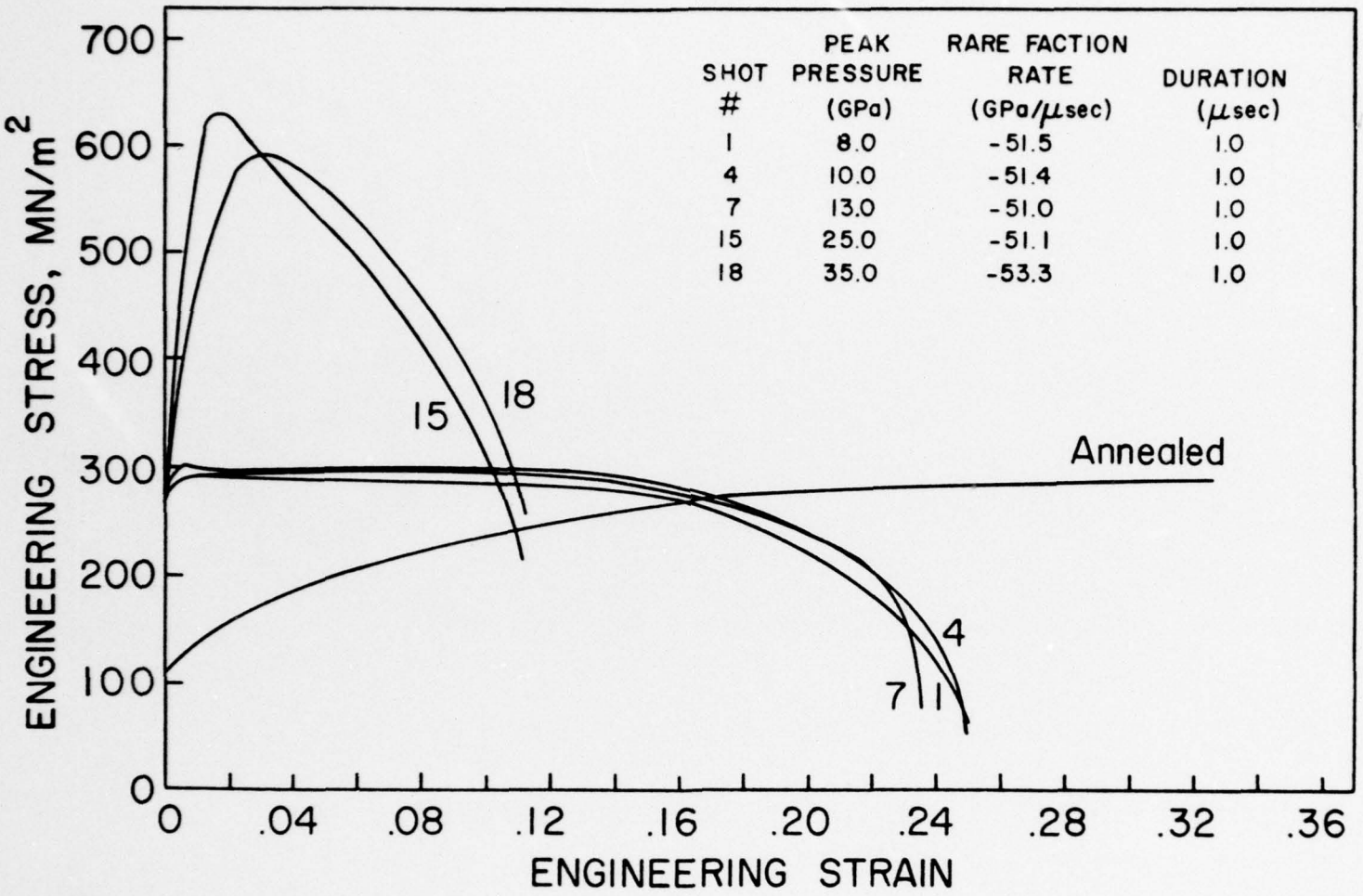

Figure 15. Engineering Stress-Strain Curves Showing the Effect of Peak Pressure on the Tensile Behavior of Armco Magnetic Ingot Iron.

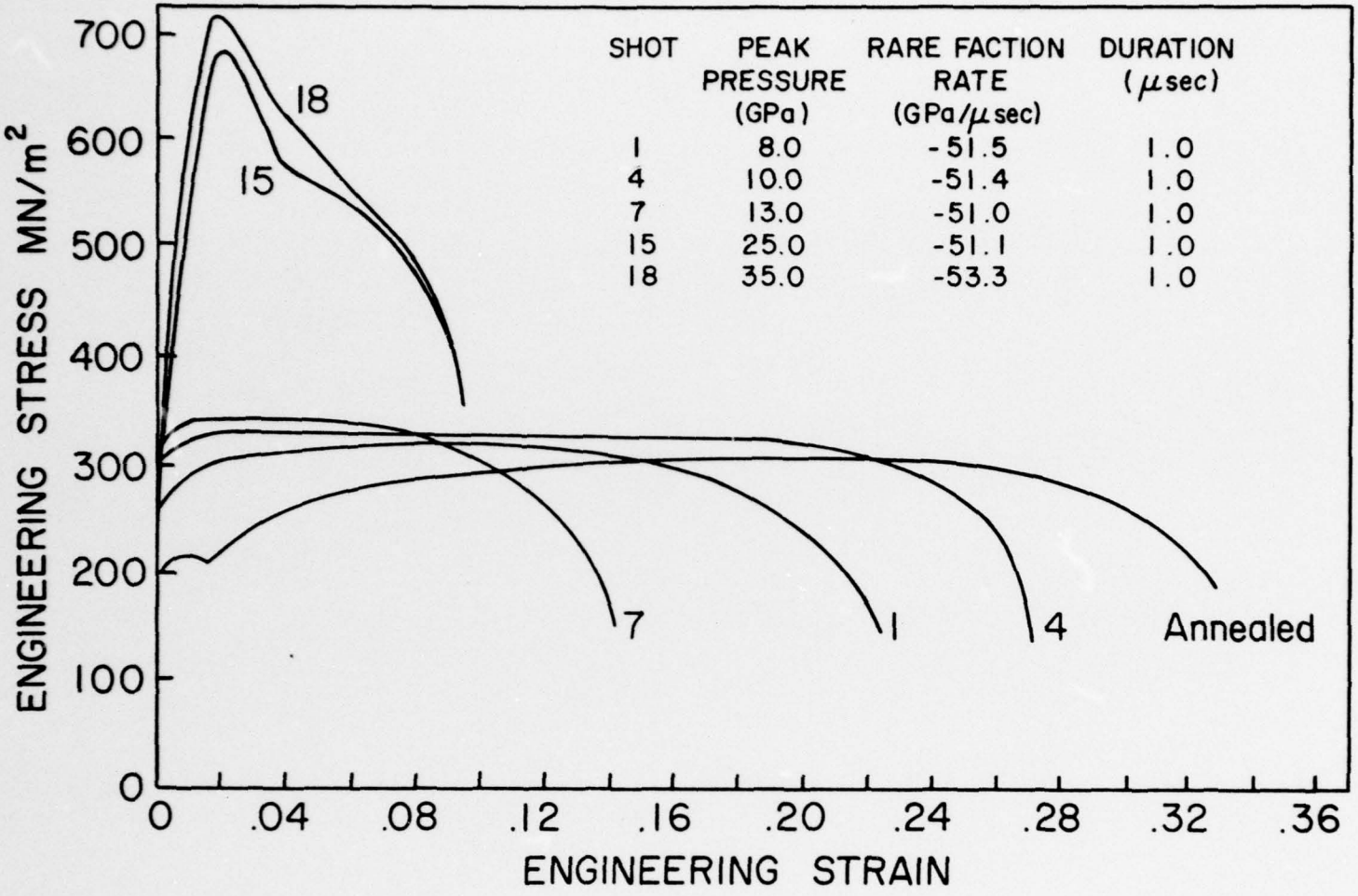

Figure 16. Engineering Stress-Strain Curves Showing the Effect of Peak Pressure on the Tensile Behavior of AISI 1008 Steel.

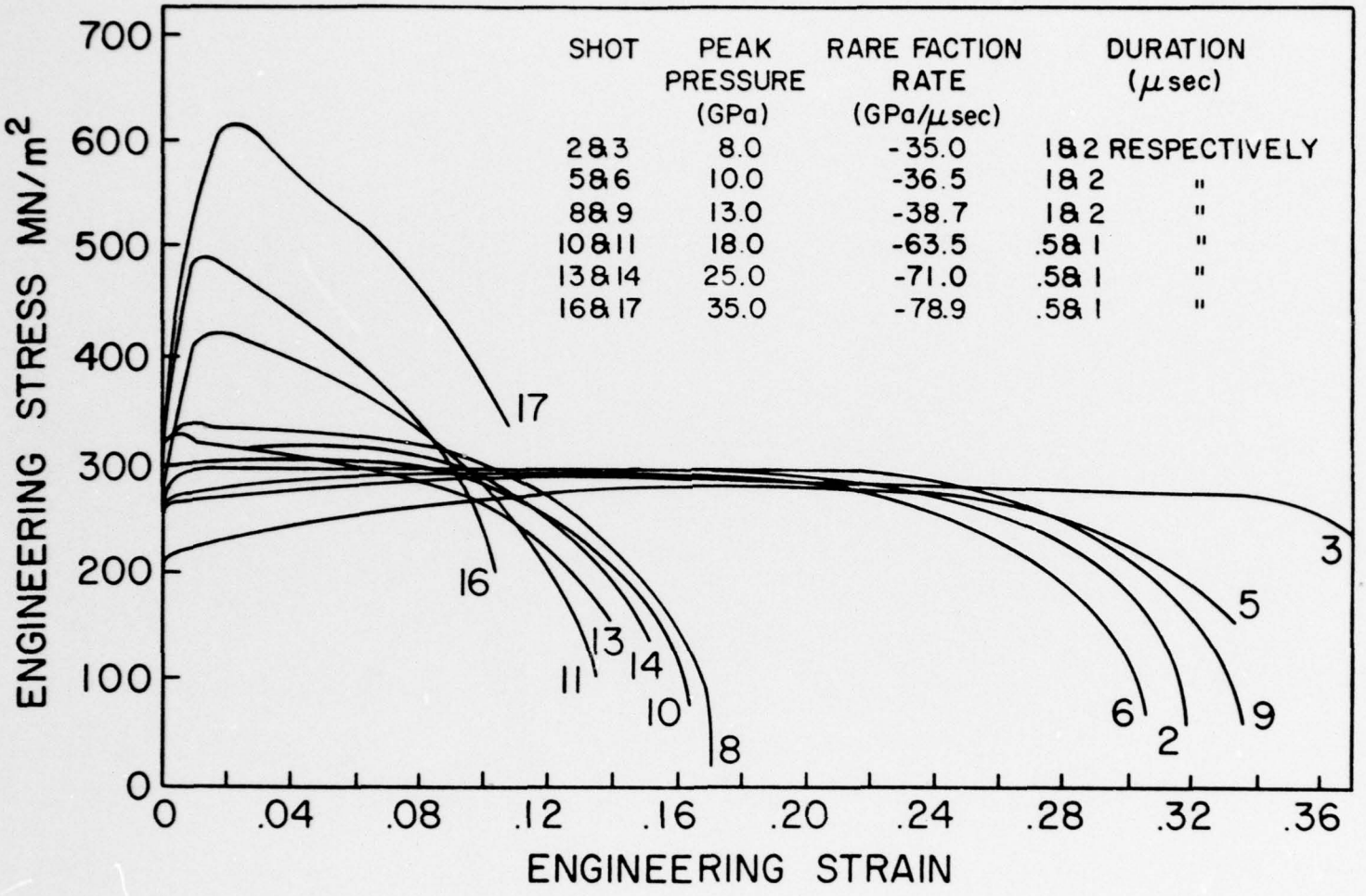

Figure 17. Engineering Stress-Strain Curves Showing the Effect of Pulse Duration on the Tensile Behavior of Magnetic Ingot Iron.

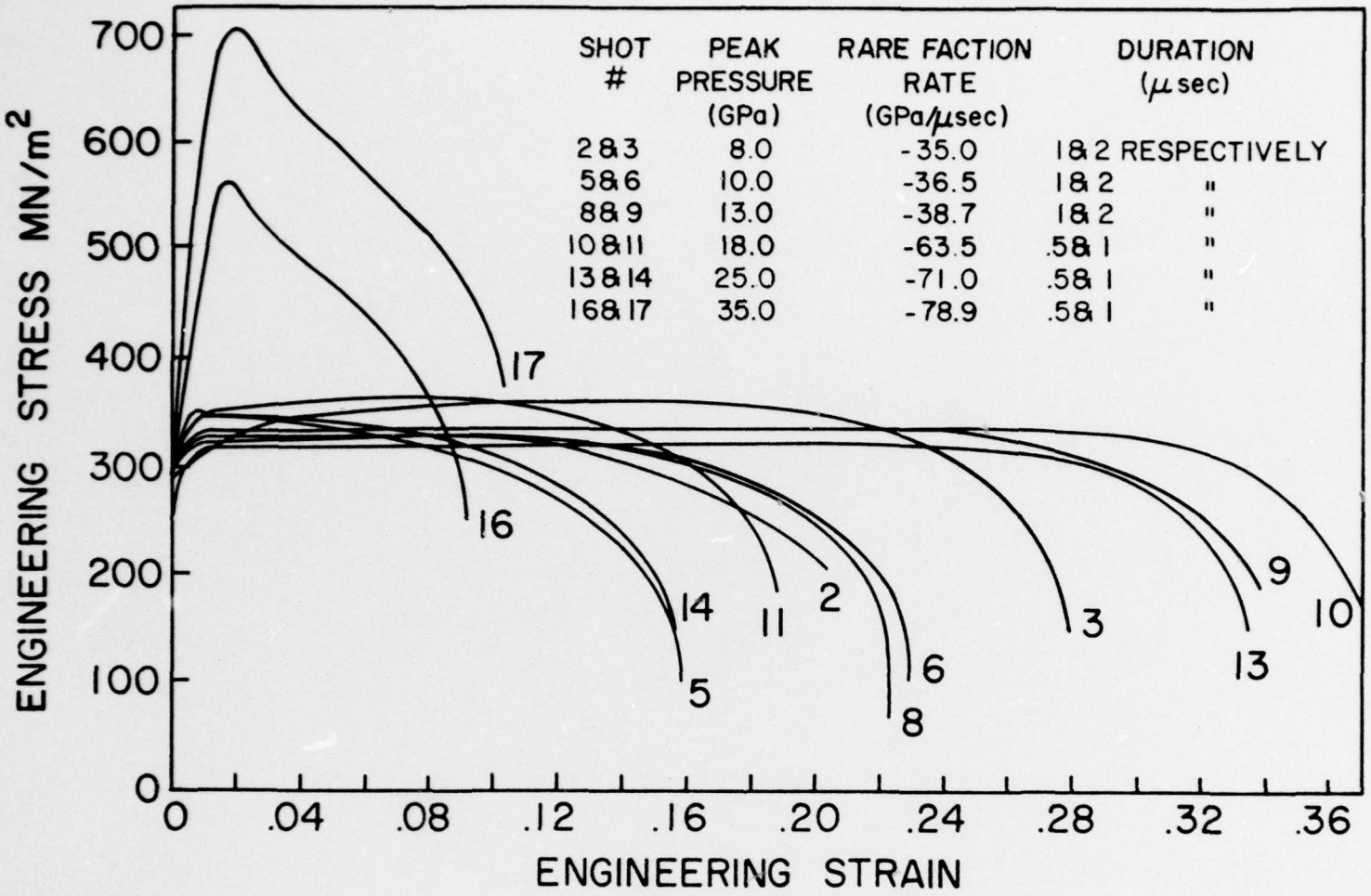

Figure 18. Engineering Stress-Strain Curves Showing the Effect of Pulse Duration on the Tensile Behavior of AISI 1008 Steel.